

NSWC/WOL/TR 76-114

12

ADA 040977
NSWC/WOL/TR 76-114

NSWC TECHNICAL REPORT C

WHITE OAK LABORATORY

ANALYTICAL MODEL FOR PREDICTING THE DYNAMIC BEHAVIOR OF CAVITIES

BY
Charles W. Smith

JULY 1976

NAVAL SURFACE WEAPONS CENTER
WHITE OAK LABORATORY
SILVER SPRING, MARYLAND 20910

- Approved for public release; distribution unlimited.

[Handwritten signature and illegible text]

AD No. _____
DDC FILE COPY

NAVAL SURFACE WEAPONS CENTER
WHITE OAK, SILVER SPRING, MARYLAND 20910

UNCLASSIFIED

SECURITY CLASSIFICATION OF THIS PAGE (When Data Entered)

REPORT DOCUMENTATION PAGE		READ INSTRUCTIONS BEFORE COMPLETING FORM
1. REPORT NUMBER NSWC/WOL/TR-76-114	2. GOVT ACCESSION NO.	3. RECIPIENT'S CATALOG NUMBER
4. TITLE (and Subtitle) Analytical Model for Predicting the Dynamic Behavior of Cavities		5. TYPE OF REPORT & PERIOD COVERED Interim FY 1976
		6. PERFORMING ORG. REPORT NUMBER
7. AUTHOR(s) Charles W. Smith		8. CONTRACT OR GRANT NUMBER(s)
9. PERFORMING ORGANIZATION NAME AND ADDRESS Naval Surface Weapons Center White Oak Laboratory White Oak, Silver Spring, Maryland 20910		10. PROGRAM ELEMENT, PROJECT, TASK AREA & WORK UNIT NUMBERS 61152N; ZR00001; ZR02301; WA0104;
11. CONTROLLING OFFICE NAME AND ADDRESS		12. REPORT DATE July 1976
		13. NUMBER OF PAGES 28
14. MONITORING AGENCY NAME & ADDRESS (if different from Controlling Office)		15. SECURITY CLASS. (of this report) UNCLASSIFIED
		15a. DECLASSIFICATION/DOWNGRADING SCHEDULE
16. DISTRIBUTION STATEMENT (of this Report) Approved for public release; distribution unlimited		
17. DISTRIBUTION STATEMENT (of the abstract entered in Block 20, if different from Report)		
18. SUPPLEMENTARY NOTES		
19. KEY WORDS (Continue on reverse side if necessary and identify by block number) Cavitation, Cavity-Running, Water-Entry Cavities		
20. ABSTRACT (Continue on reverse side if necessary and identify by block number) The first iteration in the development of an analytical model for predicting the dynamic behavior of cavities is near completion. A model to predict the cavity pressure and mass attrition needs to be developed. The predictions of the present model for the diameter and length of steady-state cavities agrees very well with experimental data. The need for reliable drag coefficients at high cavitation numbers is cited and it is recommended that future experimental work to be conducted at ARL include the measurement of drag forces in order to correct this deficiency.		

JUN 1976
ALU
C

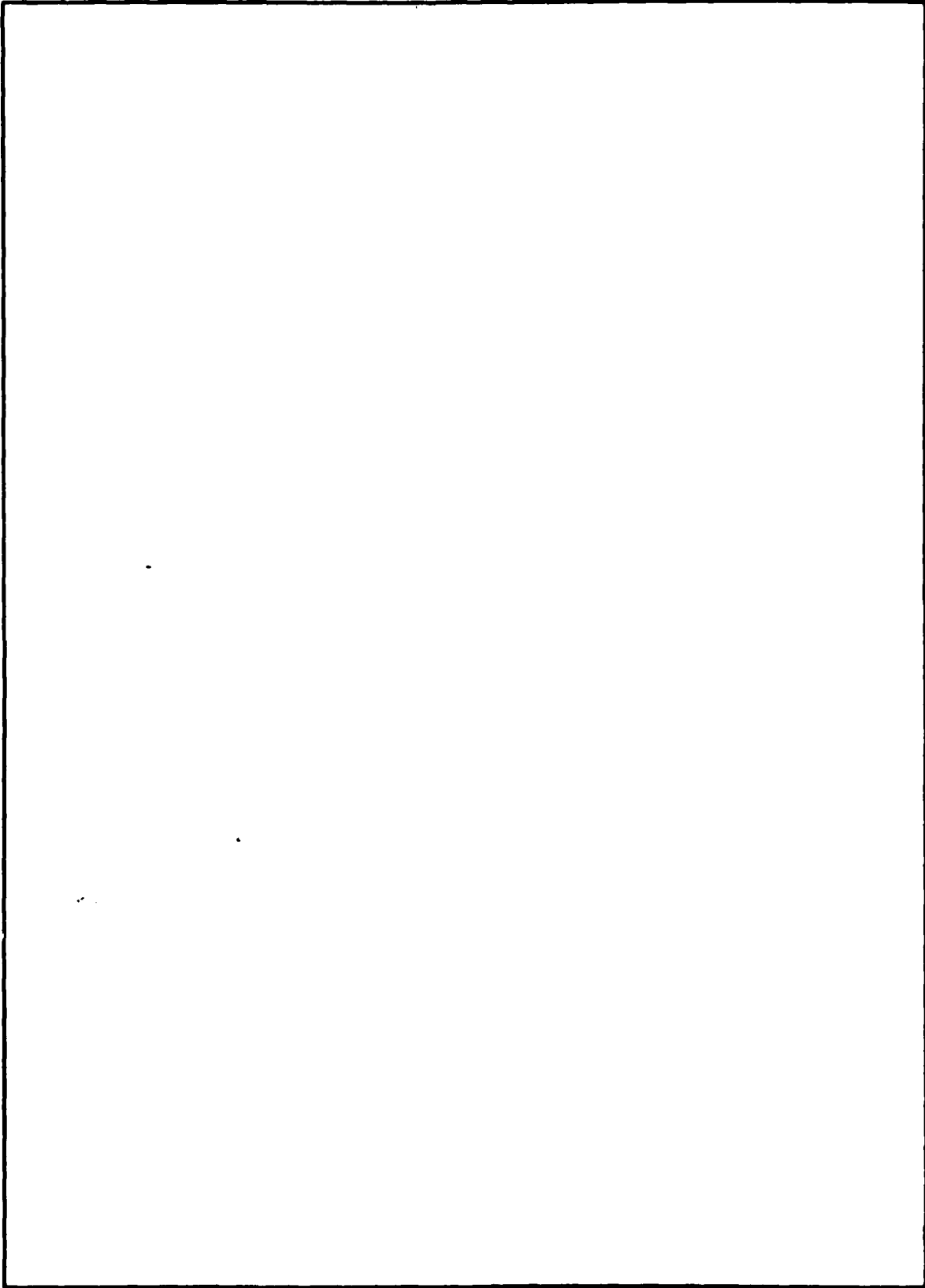
DD FORM 1473
1 JAN 73

EDITION OF 1 NOV 65 IS OBSOLETE
S/N 0102-014-6601

UNCLASSIFIED

SECURITY CLASSIFICATION OF THIS PAGE (When Data Entered)

SECURITY CLASSIFICATION OF THIS PAGE(When Data Entered)



SECURITY CLASSIFICATION OF THIS PAGE(When Data Entered)

NSWC/WOL/TR 76-114

July 1976

ANALYTICAL MODEL FOR PREDICTING THE DYNAMIC BEHAVIOR OF CAVITIES

The purpose of the present study is to develop an analytical model for predicting the dynamic behavior of cavities. The development of this model is in conjunction with an experimental program being conducted at the Applied Research Laboratory (ARL), Pennsylvania State University.

The work is being performed under funding from Dr. T. E. Peirce, Naval Sea Systems Command (SEA-03512) (SR1230102, element 61152N).

Administrative form with the following fields and markings:

- Field: THIS
- Field: DATE
- Field: BY
- Field: APPROVED/ANALYSIS
- Field: A (large handwritten letter)
- Field: (checkmark)

TABLE OF CONTENTS

	<u>Page</u>
INTRODUCTION.....	5
BACKGROUND.....	5
ELLIPSOID MODEL.....	6
DYNAMIC MODEL.....	11
CAVITY PRESSURE.....	16
RECOMMENDATIONS AND CONCLUSIONS.....	17

ILLUSTRATIONS

<u>Figure</u>	<u>Title</u>	<u>Page</u>
1	Comparison of Proposed Cavity Outlines.....	18
2	Sketch of Cavities Due to Ellipsoid and Disk Having the Same Drag Area $C_D A$	19
3	Cavity Diameter Data - Reichardt.....	20
4	Cavity Diameter Data for Disk - Waid.....	21
5	Cavity Diameter Data - Rouse and McNowen.....	22
6	Cavity Diameter Data for Disks - Eisenberg-Pond.....	23
7	Scaled Length of Cavities Due to a Disk.....	24
8	Length of Cavities for Various Nose Shapes.....	25
9	Experimental L/D Data.....	26
10	Experimental L/D Data - ARL.....	27
11	Inertial and Body Axis.....	28

TABLES

<u>Table</u>	<u>Title</u>	<u>Page</u>
1	Comparison of Results, Ellipsoid Model and Reichardt's Theoretical Formula.....	9

LIST OF SYMBOLS

A	Frontal area of cavitating body, $A = \pi r^2$
a	Major axis of ellipsoid
b	Minor axis of ellipsoid
C_d	Drag coefficient of body, based on A
C_D	Drag coefficient of 'cavity-ellipsoid', based on πb^2
C_p	Steady-state pressure coefficient, defined by equation (9)
D	Maximum diameter of cavity, $D = 2b$
d	Diameter of body, $d = 2r$
L	Length of cavity
P	Pressure on surface of 'cavity-ellipsoid'
P_c	Cavity pressure
P_∞	Pressure at infinity
R	Radial inertial coordinate, Figure 11
r	Radius of body
t	Time
t_o	Time at which the separation point (or base) arrives at a point in space, $Z = Z_o$
U	Velocity of body
V_ξ	Velocity component normal to the confocal ellipsoids in semi-elliptic coordinates (μ, ξ)
V_μ	Velocity component tangent to the confocal ellipsoids in semi-elliptic coordinates (μ, ξ)
x	Axial body coordinate, Figure 11
y	Radial body coordinate, Figure 11

LIST OF SYMBOLS (Continued)

z	Axial inertial coordinate, Figure 11
\bar{z}	Centroid of 'cavity-ellipsoid', inertial coordinate
α_0	Ellipsoidal constant, defined by equation (4)
μ, ξ	Semi-elliptic coordinates in moving frame
ξ_0	Surface of 'cavity-ellipsoid'
ρ	Mass density of fluid
σ	Cavitation number, defined by equation (8)
ϕ	Velocity potential function
ϕ_1	Potential function for moving ellipsoid
ϕ_2	Potential function for expanding ellipsoid
Superscripts	
\cdot	Derivative, $\frac{d}{dt}$
$'$	Derivative, $\frac{d}{dx}$
Subscripts	
0	Refers to value at $t = t_0$
ξ_0	Normal velocity component on the surface of the 'cavity-ellipsoid'
μ_0	Tangential velocity component on the surface of the 'cavity-ellipsoid'

INTRODUCTION

The objective of this study is to develop an analytical model for predicting the dynamic behavior of cavities formed by high-speed underwater vehicles (vapor cavities) and cavities formed during water entry and underwater launchings (air/vapor cavities). The development of this model is in conjunction with an experimental program being conducted at the Applied Research Laboratory (ARL), Pennsylvania State University. Recent experimental work investigating cavities formed by cones in a water tunnel at ARL is reported in reference (1). The use of a water tunnel is advantageous in that the mass attrition rates can be determined for different size cavities by measuring the air flow rate feeding the cavity.

BACKGROUND

The need to predict the trajectory of cavity-running underwater vehicles has been given emphasis by recent development effort. To successfully predict the trajectory of a vehicle riding in a cavity requires a knowledge of the forces acting on the vehicle which are influenced by the presence of a cavity. Water entry and underwater launching are areas of weapon delivery where the presence of a cavity has a significant effect on the trajectory of a vehicle.

High-speed underwater vehicles produce a trailing vapor cavity when the minimum local pressure on the vehicle is less than the water vapor pressure. At water entry, high-speed vehicles produce an open air filled cavity. Upon cavity closure, the cavity often continues to expand and then collapse to form one or more stationary cavities and a moving trailing cavity which behaves in the same manner as a vapor cavity. In fact, this trailing cavity can become a vapor cavity after the entrapped air has been removed by attrition.

The pressure within these cavities and their size and shape have a significant effect on the performance and trajectory of the vehicle. The most pronounced effect is on the drag. When a vehicle is trailed by a cavity, the drag on the vehicle (other than friction drag which can be significant for long slender bodies) is primarily due to the dynamic pressure on the forebody and the low cavity pressure on the afterbody. There is no pressure recovery on the afterbody until the cavity closes on the afterbody. An unstabilizing lift force is produced on the forebody when an angle of attack exists. A lift force can also be produced on the afterbody when it contacts the cavity wall. Predicting these factors can best be accomplished by first predicting the behavior and configuration of the cavity.

¹Kim, J. H. and Holl, J. W., "Water Tunnel Simulation Study of the Later Stages of Water Entry of Conical Head Bodies", Applied Research Laboratory, Pennsylvania State University, Technical Memorandum 75-177, 18 Jun 1975

ELLIPSOID MODEL

Münzer and Reichardt (Ref. (2)) and Waid (Ref. (3)) described the cavity outline as a generalized ellipsoid. Münzer and Reichardt derived their ellipsoid from a theoretical constant-pressure surface while Waid obtained his experimentally from cavities due to a disk. A study was made by May (Ref. (4)) to determine how widely these two representations and a true ellipsoid differed. May gave a sketch, copied in Figure 1, showing a comparison of the generalized ellipsoid formulae using an axis ratio of six. The outlines are indistinguishable over most of their length and differ only in the vicinity of the nose.

Reichardt (Ref. (5)) derived by source-sink methods a theoretical formula for the cavity diameter, D

$$\frac{D}{d} = \left[\frac{C_d}{\sigma - .132\sigma^{8/7}} \right]^{1/2} \quad (1)$$

which shows the diameter to be a function of only the cavity-running drag coefficient and the cavitation number. To illustrate why the form of equation (1) is possible he gave a sketch, copied from reference (4) in Figure 2, which shows the outlines of the cavities formed by an ellipsoidal nose and a disk with the same drag area, $C_d A$. The cavities, having the same diameter, differ in contour only in the vicinity of the nose.

Since an ellipsoid, for which potential flow solutions are available, appears to be a reasonable choice for a model describing the cavity shape, the following approach was taken. It is assumed that the pressure drag force on an arbitrary nose shape which forms a cavity is equal to the pressure drag force on the forebody of an ellipsoid which has a minimum local pressure equal to the cavity pressure, P_c .

²Münzer, H. and Reichardt, H., "Rotational Symmetrical Source-Sink Bodies with Predominantly Constant Pressure Distributions", Armament Research Establishment, Ministry of Supply, Fort Halstead, Kent, England, Trans. 1/50, 1950

³Waid, R. L., "Cavity Shapes for Circular Disks at Angles of Attack", California Institute of Technology Hydrodynamics Laboratory, Report E-73.4, 1957

⁴May, A., "Water Entry and the Cavity-Running Behavior of Missiles", Naval Surface Weapons Center, White Oak Laboratory, SEAHAC TR 75-2, 1975

⁵Reichardt, H., "The Laws of Cavitation Bubbles at Axially Symmetrical Bodies in a Flow", Ministry of Aircraft Production Volkenrode, MAP-VG, Reports and Translations 766, ONR, 1946

The local pressure, P , on the surface of an ovary ellipsoid, $a > b$

$$\left(\frac{x}{a}\right)^2 + \left(\frac{y}{b}\right)^2 = 1 \quad (2)$$

can be expressed (Ref. (6))

$$P - P_\infty = \frac{1}{2} \rho U^2 \left(\frac{2}{2 - \alpha_0}\right)^2 \left[\frac{(y')^2}{1 + (y')^2} - \frac{\alpha_0 (4 - \alpha_0)}{4} \right] \quad (3)$$

where

$$\alpha_0 = 2(\xi_0^2 - 1) \left[\frac{1}{2} \xi_0 \ln \frac{\xi_0 + 1}{\xi_0 - 1} - 1 \right] \quad (4)$$

$$\xi_0^2 = \frac{a^2}{a^2 - b^2} \quad (5)$$

$$y' = \frac{dy}{dx} \quad (6)$$

The minimum pressure, $P = P_c$, occurs when $y' = 0$

$$P_c - P_\infty = \frac{1}{2} \rho U^2 \left[1 - \left(\frac{2}{2 - \alpha_0}\right)^2 \right] \quad (7)$$

The cavitation number is defined

$$\sigma = \frac{P_\infty - P_c}{\frac{1}{2} \rho U^2} = \left(\frac{2}{2 - \alpha_0}\right)^2 - 1 \quad (8)$$

⁶Smith, C. W. and Guala, J. R., "Axisymmetric Ellipsoids in Ideal Fluids", Naval Surface Weapons Center, White Oak Laboratory, NOLTR 73-155, 1 Aug 1973

and the local pressure coefficient is defined

$$C_p = \frac{P - P_\infty}{\frac{1}{2} \rho U^2} = \frac{(1 + \sigma) (y')^2}{1 + (y')^2} - \sigma \quad (9)$$

Integrating over the surface of the forebody of an ellipsoid, $0 \leq x \leq a$, the drag force is obtained

$$\begin{aligned} \text{Drag} &= 2\pi \int_0^b (P - P_c) y dy \\ &= 2\pi \int_0^b \left[(P - P_\infty) + (P_\infty - P_c) \right] y dy \\ &= \frac{1}{2} \rho U^2 \pi b^2 C_D \end{aligned} \quad (10)$$

where C_D denotes the pressure drag coefficient of an ellipsoid based on the maximum frontal area, πb^2

$$C_D = (1 + \sigma) (\xi_0^2 - 1) \left[\xi_0^2 \ln \frac{\xi_0^2}{\xi_0^2 - 1} - 1 \right] \quad (11)$$

Equating the drag on the nose shape forming the cavity to the drag on the 'cavity-ellipsoid'

$$\text{Drag} = \frac{1}{2} \rho U^2 \pi b^2 C_D = \frac{1}{2} \rho U^2 \pi r^2 C_d \quad (12)$$

The following expression is obtained for the cavity diameter

$$\frac{D}{d} = \left[\frac{C_d}{C_D} \right]^{1/2} \quad (13)$$

where

$$\begin{aligned} D &= 2b, \text{ cavity diameter} \\ d &= 2r, \text{ body diameter} \end{aligned}$$

Table 1
 Comparison of Results
 Ellipsoid Model and Reichardt's Theoretical Formula

σ	$\left(\frac{D}{d}\right)^2 / C_d$	
	Ellipsoid Model, Equation (15)	Reichardt, Equation (14)
.001	1011.	1015.
.0021	500.	502.
.0042	250.	251.
.0069	153.7	154.4
.0130	78.6	79.0
.0244	44.2	44.4
.036	30.2	30.3
.049	22.1	22.2
.059	18.4	18.5
.082	13.5	13.5
.105	10.5	10.5
.170	6.55	6.56
.207	5.39	5.41
.259	4.32	4.34
.318	3.52	3.54
.405	2.77	2.79
.500	2.24	2.27
.585	1.91	1.94
.700	1.60	1.63
.858	1.30	1.34
1.09	1.02	1.06

Rearranging equations (1) and (13) as follows, for equation (1)

$$\frac{D^2}{C_d d^2} = \frac{1}{\sigma - .132\sigma^{8/7}} \quad (14)$$

for equation (13)

$$\frac{D^2}{C_d d^2} = \frac{1}{C_D} \quad (15)$$

and comparing the results, it is seen that the results, as shown in Table 1, are nearly identical, especially for low cavitation numbers. To facilitate the calculations for equation (15) the axis ratio, a/b , was first selected, α was then calculated from equations (4) and (5), the cavitation number, σ , from equation (8) and C_D from equation (11). Since the agreement between equations (14) and (15) is so close, a more direct method to obtain C_D can be formulated by equating equations (14) and (15). The concept of the 'cavity ellipsoid', however, is retained since it permits a more direct treatment for the dynamic behavior of the cavity.

Figures 3 through 6, copied from reference (4), show the scaled diameter of cavities plotted from data obtained by Reichardt (Ref. (5)), Waid (Ref. (3)), Rouse and McNowen (Ref. (7)) and Eisenberg-Pond (Ref. (8)). Equation (15), plotted in these figures, appears to be a good representation of the data.

Figures 7 through 9, obtained from reference (4), show data for the lengths of cavities. The cavity half-lengths were measured from the base (or separation point) to the point of maximum cavity diameter. The ratios of the cavity length to cavity diameter, D , and body diameter, d , can thus be expressed:

$$\frac{L}{D} = \frac{L}{2b} = \frac{x}{b} = \frac{x}{a} \frac{a}{b} \quad (16)$$

$$\frac{L}{d} = \frac{L}{D} \frac{D}{d} \quad (17)$$

where x/a denotes the position of the separation point on the cavitating nose within the assumed 'cavity ellipsoid'. As shown in Figure 2, the separation point is not located at the tip ($x/a = 1$) of the 'cavity ellipsoid'. In correlating the data for the length of cavities formed by a disk, the following expression was obtained:

⁷Rouse, H. and McNowen, J. S., "Cavitation and Pressure Distribution; Head Forms at Zero Angle of Yaw", State University of Iowa, Studies in Eng. Bull. 32, 1948

⁸Eisenberg, P. and Pond, H. L., "Water Tunnel Investigations of Steady-State Cavities", David Taylor Model Basin Report 668, 1948

$$\frac{x}{a} = \left[\frac{\frac{2}{3} \alpha_o \left(\frac{a}{b}\right)^2}{1 + \frac{2}{3} \alpha_o \left(\frac{a^2 - b^2}{b^2}\right)} \right]^{1/2} \quad (18)$$

Using equations (18), (13), and (5), equations (16) and (17) can be expressed:

$$\frac{L}{D} = \frac{\xi_o^2}{\xi_o^2 - 1} \left[\frac{\frac{2}{3} \alpha_o (\xi_o^2 - 1)}{\frac{2}{3} \alpha_o + (\xi_o^2 - 1)} \right]^{1/2} \quad (19)$$

$$\frac{L}{d\sqrt{C_d}} = \frac{L}{D\sqrt{C_D}} \quad (20)$$

Equation (20) is plotted in Figures 7 and 8 which show the scaled length of cavities as a function of cavitation number. In Figure 7 data for cavities due to a disk are plotted. In a similar manner data for various nose shapes are plotted in Figure 8. The agreement with equation (20) is shown to be excellent. In Figure 9 experimental L/D data and equation (19) are plotted. The agreement with the experimental data is shown to be excellent in the region for $\sigma < 0.2$. In the region $\sigma \geq 0.2$, equation (19) appears to be an upper bound on the data which exhibits considerable scatter. The scatter of the data in Figure 9 may be due to the dependence of L/D on the nose shape (slope at the separation point or C_d of the cavitating nose).

Recent experimental L/D data obtained at ARL (Ref. (1)) for 18- and 45-degree cones with cylindrical afterbodies, shown in Figure 10, clearly show a strong dependence on the nose shape. The need for further study is clearly evident. The dependence of the cavity L/D on the nose shape suggests, from equation (20), the dependence of the scaled cavity length, and/or, from equation (13), the dependence of the scaled cavity diameter on the nose shape. The agreement with various nose shapes, shown in Figure 8 for the scaled length of cavities, and in Figures 3 and 5 for the scaled diameters of cavities, may be misleading. The experimental data in these figures were scaled using cavitating drag coefficients. Except for the disk, drag data are sparse in the region for $\sigma > 0.2$ and drag coefficients obtained from these data should not be considered reliable enough to establish a firm trend.

DYNAMIC MODEL

The velocity potential for an axisymmetric ellipsoid is readily obtained, as shown in reference (9), using dimensionless ovary semi-elliptic coordinates (u, v) . The transformation equations are:

⁹Durand, W. F., Aerodynamic Theory, Vol. I, Div. C, Chap VII, Dover Publications, Inc., New York, 1963

$$x = \sqrt{a^2 - b^2} \mu \xi \quad (21)$$

$$y = \sqrt{a^2 - b^2} \sqrt{1 - \mu^2} \sqrt{\xi^2 - 1} \quad (22)$$

where

$$-1 \leq \mu \leq +1 \quad \text{and} \quad \xi \geq 1 \quad (23)$$

The coordinate ξ , which can be written:

$$\xi = \sqrt{\frac{a^2 + v}{a^2 - b^2}} \quad , \quad v \geq 0 \quad (24)$$

defines the surfaces of confocal ellipses with the foci at

$$x = \pm \sqrt{a^2 - b^2} \quad , \quad y = 0 \quad (25)$$

The surface of the 'cavity ellipsoid' is defined by the coordinate ξ_0 , for $v = 0$

$$\xi_0 = \xi(v = 0) = \frac{a}{\sqrt{a^2 - b^2}} \quad (26)$$

and the Cartesian coordinates on the surface, ξ_0 , become:

$$x = a\mu \quad (27)$$

$$y = b \sqrt{1 - \mu^2} \quad (28)$$

The velocity potential function for an axisymmetric ellipsoid moving with an axial velocity, U , in an infinite ideal fluid can be expressed, Ref. (9).

$$\phi_1 = \Lambda_1 U \left[\frac{1}{2} \ln \frac{\xi + 1}{\xi - 1} - \frac{1}{\xi} \right] \quad (29)$$

where

$$\Lambda_1 = \frac{2(b_0)}{(2 - \xi_0^2)} \xi_0 \sqrt{\xi_0^2 - 1} \quad (30)$$

For an expanding (or contracting) ellipsoid with the fluid velocity everywhere normal to the confocal ellipsoids, the velocity potential function can be expressed:

$$\phi_2 = \frac{1}{2} A_2 \ln \frac{\xi + 1}{\xi - 1} \quad (31)$$

where

$$A_2 = b \dot{b} \xi_0 \quad (32)$$

and

$$a\dot{b} = \dot{a}b + \frac{a}{b} = \frac{a_0}{b_0}, \text{ Constant} \quad (33)$$

The velocity potential function for a moving and expanding ellipsoid can now be obtained by adding:

$$\phi = \phi_1 + \phi_2 \quad (34)$$

The fluid velocity component normal to the confocal ellipsoids is:

$$v_\xi = - \frac{1}{\sqrt{a^2 - b^2}} \sqrt{\frac{\xi^2 - 1}{\xi^2 - \mu^2}} \frac{\partial \phi}{\partial \xi} \quad (35)$$

and the tangential fluid velocity component is:

$$v_\mu = - \frac{1}{\sqrt{a^2 - b^2}} \sqrt{\frac{1 - \mu^2}{\xi^2 - \mu^2}} \frac{\partial \phi}{\partial \mu} \quad (36)$$

On the surface of the 'cavity ellipsoid' the fluid velocity components are:

$$v_{\xi_0} = v_\xi \Big|_{\xi=\xi_0} = U \mu \sqrt{\frac{\xi_0^2 - 1}{\xi_0^2 - \mu^2}} + \frac{\dot{b} \xi_0}{\sqrt{\xi_0^2 - \mu^2}} \quad (37)$$

$$v_{\mu_0} = v_\mu \Big|_{\xi=\xi_0} = - \frac{a_0 U \xi_0}{(2 - \nu_0)} \sqrt{\frac{1 - \mu^2}{\xi_0^2 - \mu^2}} \quad (38)$$

To determine the configuration of a dynamic cavity, consecutive 'cavity disks' of finite thickness can be tracked in inertial coordinates (Z, R) , Figure 11. The initial properties of the 'cavity disk' (a_0, b_0) can be determined using the instantaneous velocity (U_0) and the cavity pressure (P_c) at the moment $(t = t_0)$ the 'cavity disk' separates from the cavitating nose. The radius, R , and position, Z , of the 'cavity disk' are:

$$R = y = b\sqrt{1 - \mu^2} \quad (39)$$

$$z - \bar{z}_0 = x + \int_{t_0}^t U d\tau = a\mu + \int_{t_0}^t U d\tau \quad (40)$$

where \bar{z}_0 is the centroid of the ellipsoid which contains the 'cavity disk' formed at $t = t_0$.

Taking the time derivative of equation (40):

$$\dot{z} = \dot{x} + U = a\dot{\mu} + \dot{a}\mu + U \quad (41)$$

It is seen that:

$$\dot{z} = 0 \quad (42)$$

and

$$\dot{x} = a\dot{\mu} = -U \quad (43)$$

when the cavity is not expanding, $\dot{a} = 0$. Thus,

$$\dot{\mu} = -\frac{U}{a} \quad (44)$$

and for an expanding cavity:

$$\dot{z} = \dot{a}\mu \quad (45)$$

To obtain an expression for \dot{b} , the change in the kinetic energy of the fluid flow field must be considered. The kinetic energy of the fluid is:

$$T = -\frac{1}{2} \rho \int_{\xi = \xi_0} \int \phi \frac{\partial \phi}{\partial \eta} dS \quad (46)$$

where, on the surface, $\xi = \xi_0$

$$dS = 2\pi(a^2 - b^2) \sqrt{(\xi_0^2 - \mu^2)(\xi_0^2 - 1)} d\mu \quad (47)$$

$$\frac{\partial \phi}{\partial \eta} = \frac{1}{\sqrt{a^2 - b^2}} \sqrt{\frac{\xi_0^2 - 1}{\xi_0^2 - \mu^2}} \frac{\partial \phi}{\partial \xi} \Big|_{\xi = \xi_0} \quad (48)$$

Therefore:

$$T = -\rho \pi b \sqrt{\xi_0^2 - 1} \int_{-1}^{+1} \left[\phi \frac{\partial \phi}{\partial \xi} \right]_{\xi=\xi_0} d\mu \quad (49)$$

$$T = \frac{1}{2} \rho U^2 \bar{V} K_1 + \frac{3}{2} \rho b^2 \bar{V} K_2 \quad (50)$$

where:

$$\bar{V} = \frac{4}{3} \pi a b^2, \text{ cavity volume} \quad (51)$$

$$K_1 = \frac{\alpha_0}{(2 - \alpha_0)} \quad (52)$$

$$K_2 = \frac{1}{2} \xi_0 \ln \frac{\xi_0 + 1}{\xi_0 - 1} \quad (53)$$

The momentum of the fluid in the forward direction does not change. Therefore,

$$\frac{d}{dt} [K_1 \rho \bar{V} U] = \frac{d}{dt} \left[\frac{\partial T}{\partial U} \right] = 0 \quad (54)$$

Thus,

$$\frac{d}{dt} [U \bar{V}] = 0 \quad (55)$$

$$\frac{d}{dt} [U b^3] = \dot{U} b^3 + 3 U b^2 \dot{b} = 0 \quad (56)$$

and

$$\dot{U} = - \frac{3U\dot{b}}{b} = - \frac{3U\dot{a}}{a} \quad (57)$$

Since $a\dot{b} = \dot{a}b$, from equation (33).

The change in the kinetic energy due to the expansion of the cavity can be written:

$$(\bar{P} - P_{\infty}) \frac{d\bar{V}}{dt} = \frac{dT}{dt} \quad (58)$$

where \bar{P} is the average pressure on the surface of the 'cavity ellipsoid'. Performing the differentiation and rearranging, equation (58) becomes:

$$\frac{\bar{P} - P_{\infty}}{\rho} = K_2 \left[b \ddot{b} + \frac{3}{2} \dot{b}^2 \right] - \frac{1}{2} K_1 U^2 \quad (59)$$

Defining the cavity pressure when \ddot{b} and $\dot{b} = 0$, from equation (7):

$$\frac{P_{C_0} - P_{\infty}}{\rho} = -\frac{1}{2} U^2 \left[\left(\frac{2}{2 - t_0} \right)^2 - 1 \right] \quad (60)$$

instead of using the average pressure on the surface when \ddot{b} and $\dot{b} = 0$, from equation (59)

$$\frac{\bar{P}_0 - P_{\infty}}{\rho} = -\frac{1}{2} U^2 K_1 \quad (61)$$

equation (59) becomes:

$$\frac{\bar{P} - P_{C_0}}{\rho} = K_2 \left[b \ddot{b} + \frac{3}{2} \dot{b}^2 \right] \quad (62)$$

Solving for \ddot{b}

$$\ddot{b} = -\frac{3}{2} \frac{\dot{b}^2}{b} + \frac{\bar{P} - P_{C_0}}{\rho b K_2} \quad (63)$$

an expression for \dot{b} can be obtained:

$$\dot{b} = \int_{t_0}^t \ddot{b} \, d\tau \quad (64)$$

CAVITY PRESSURE

A cavity pressure model for predicting the cavity pressure and mass attrition rate needs to be developed. The model will need to incorporate an air flow model for open cavities and an energy model for expanding cavities which are often experienced during water entry after cavity closure. An attempt to correlate the mass attrition data (air flow coefficients) contained in Reference (1) with one correlation for 18- and 45-degree cones using the cavitating drag coefficient

as a parameter was unsuccessful due to the lack of reliable drag coefficients at high cavitation numbers. It is believed that the mass attrition occurs primarily at the base (tail) of the cavity and is in some manner proportional to the drag force which creates the cavity. Correlation of mass attrition data in this manner may eliminate the need for a separate correlation for each drag shape.

RECOMMENDATIONS AND CONCLUSIONS

The predictions of the model for the diameter and length of steady-state cavities agrees very well with experimental data except for the dependence of the cavity L/D on nose shape. The cavity length, as shown in Figure 10 and also noted in reference (1), was found to be strongly influenced by the body shape at high cavitation numbers. The drag coefficient is a likely parameter for correlating the cavity length and mass attrition rate. Since drag data at high cavitation numbers is sparse, it is recommended the future tests conducted at ARL include the measurement of the drag force. The use of a water tunnel is particularly appropriate since steady-state conditions can be maintained during the measurement of the drag force. Future tests should also consider additional nose shapes with and without an afterbody. This recommendation is made in order to obtain reliable correlations which hopefully will apply to any drag shape (given the drag coefficient) and include the effect of cavity closure on the afterbody.

Additional work on the analytical model is required. A model for predicting the cavity pressure needs to be developed and the effect of the free surface should be included. A digital program also needs to be written and the predicted behavior of the cavities compared with future experimental results and the results contained in reference (1). The experimental results contained in references (10) and (11) for the cavity shape and pressure during water entry should also be compared with the predictions of the analytical model. As the development of the model progresses, the need for dynamic water-entry tests, and the test conditions, can be better identified.

¹⁰ Aronson, P. M., "An Experimental Investigation of Cavity Pressure Scaling and Drag Coefficients Encountered in the Water Entry of Vehicles", PhD Thesis, University of Maryland, 1975

¹¹ Abelson, H. I., "The Behavior of the Cavity Formed by a Projectile Entering the Water Vertically", PhD Thesis, University of Maryland, 1969

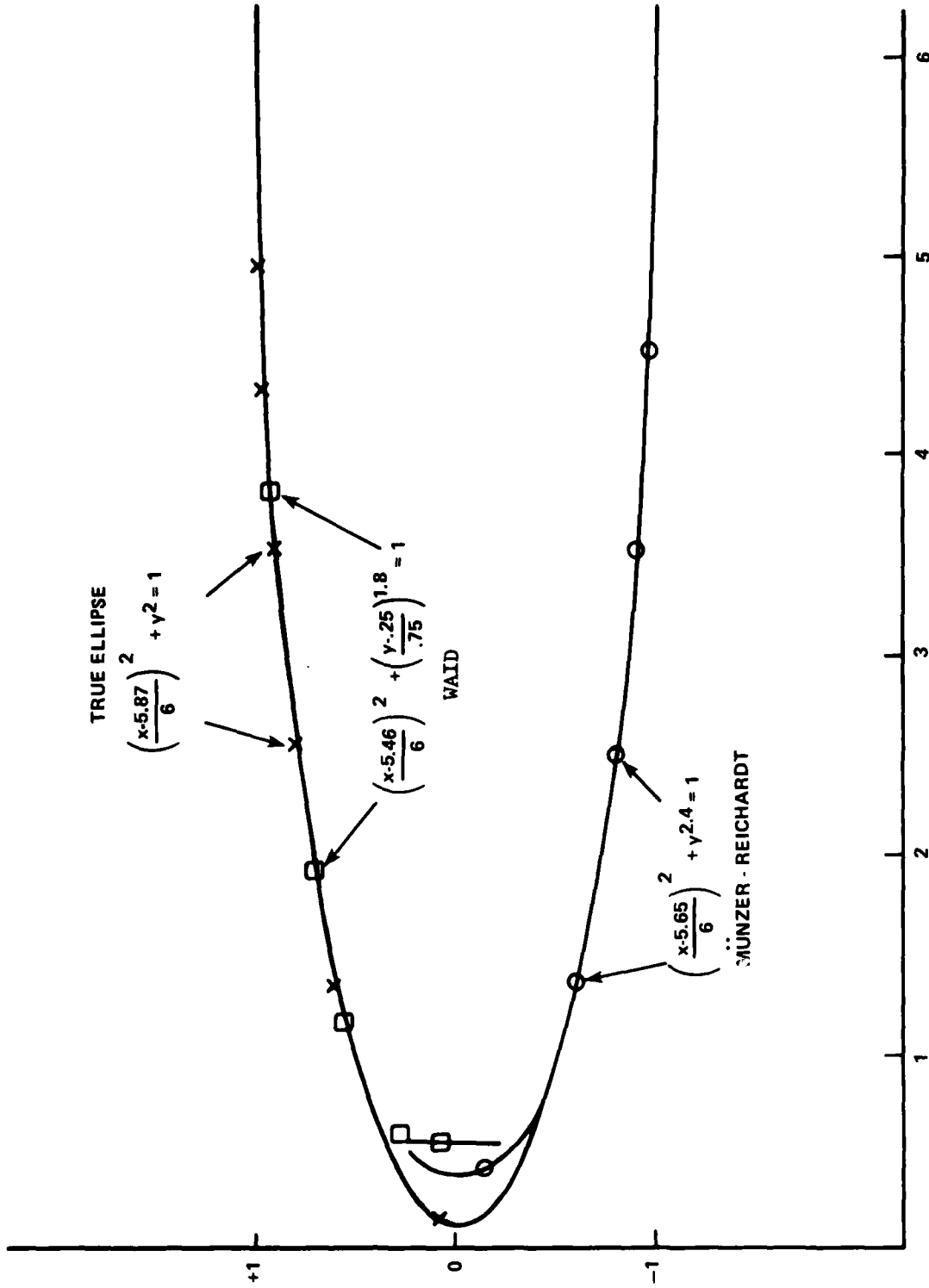


FIG. 1 COMPARISON OF PROPOSED CAVITY OUTLINES, REF (4)

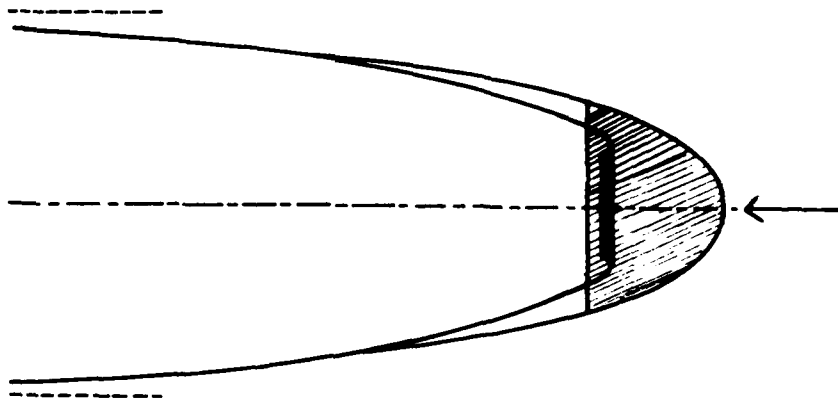


FIG. 2 SKETCH OF CAVITIES DUE TO ELLIPSOID AND DISK HAVING THE SAME DRAG AREA C_dA . AFTER REICHARDT REF (5)

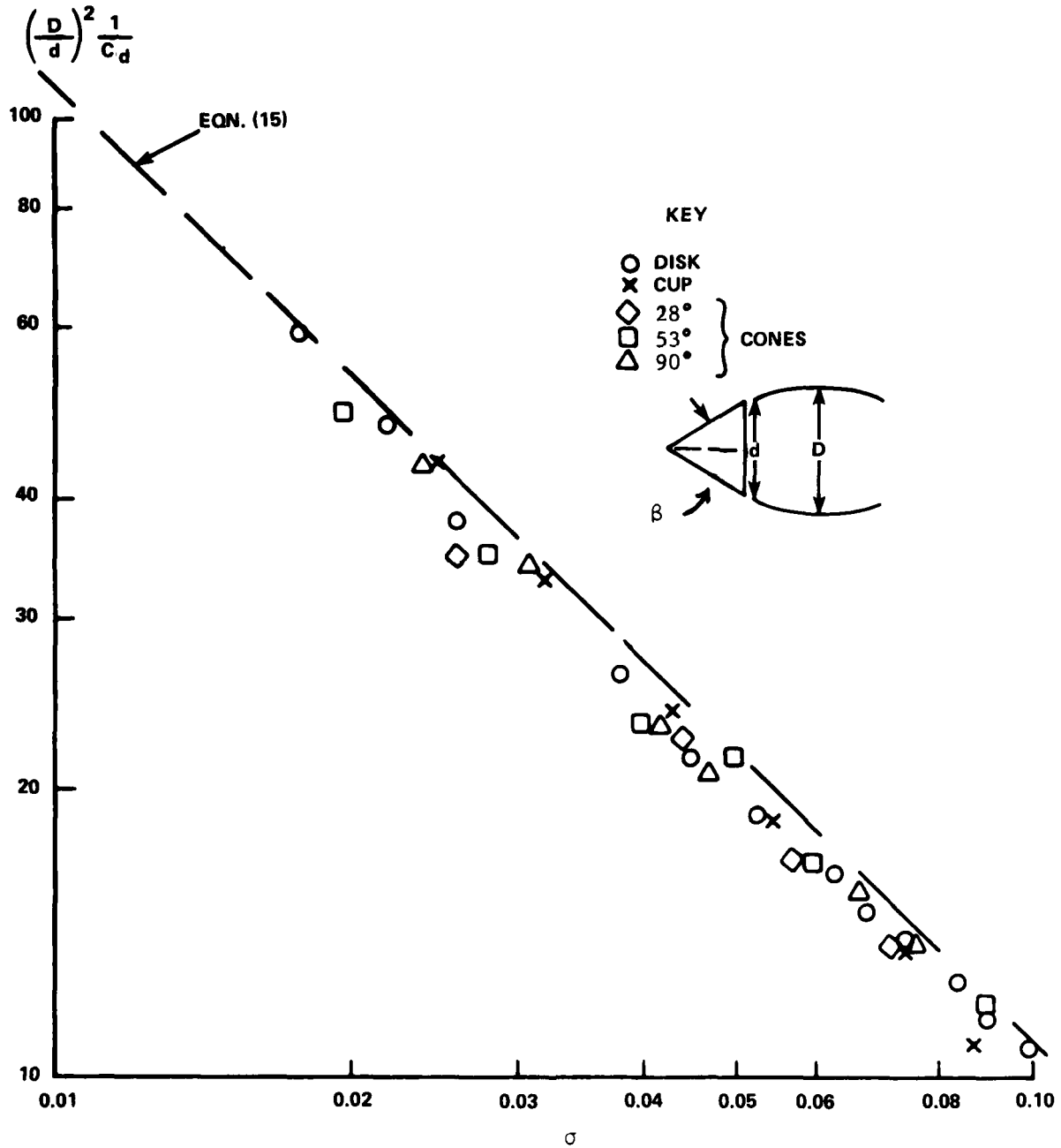


FIG. 3 CAVITY DIAMETER DATA - REICHARDT REF (5)

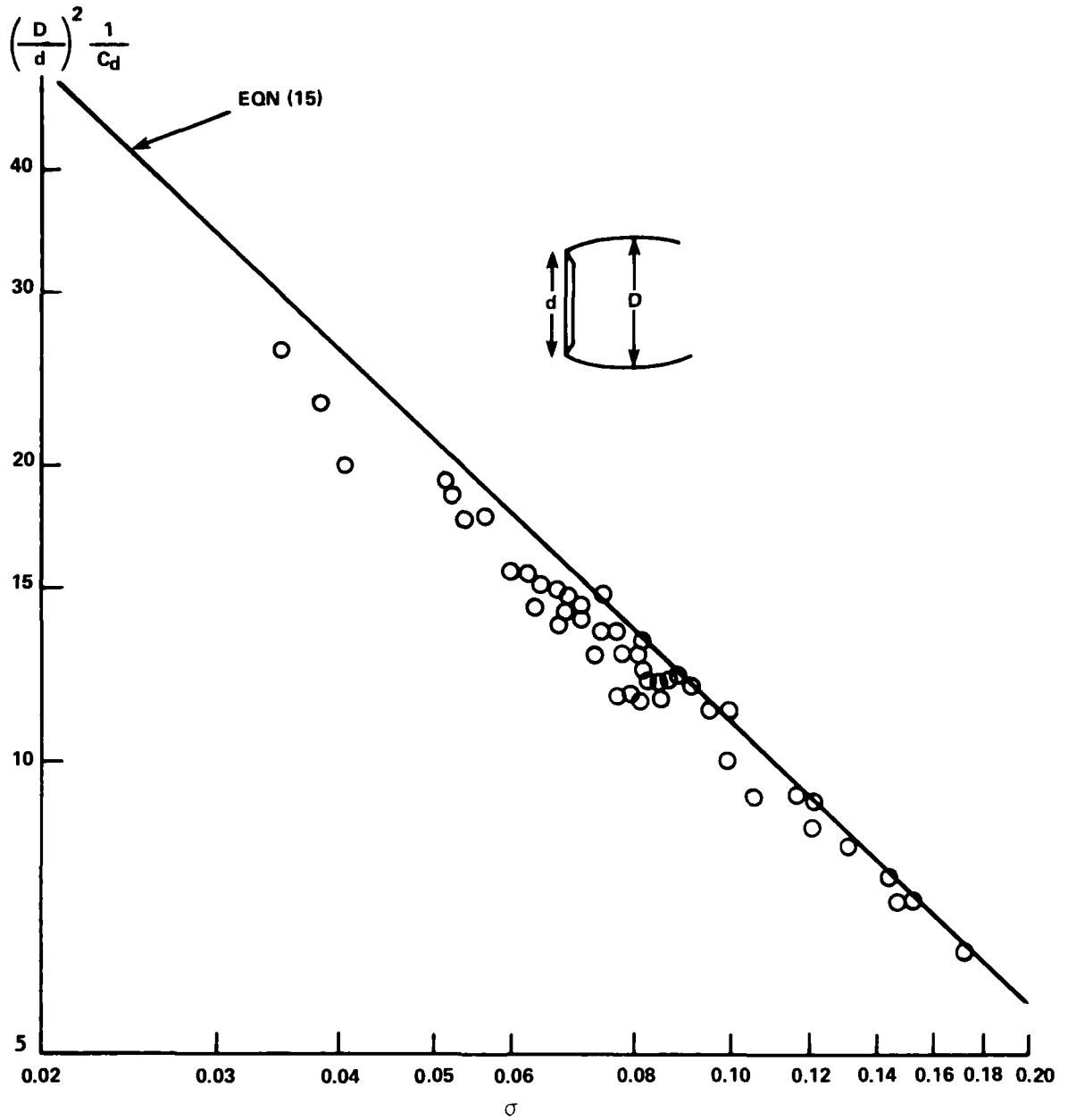


FIG. 4 CAVITY DIAMETER DATA FOR DISK - WAID REF (3)

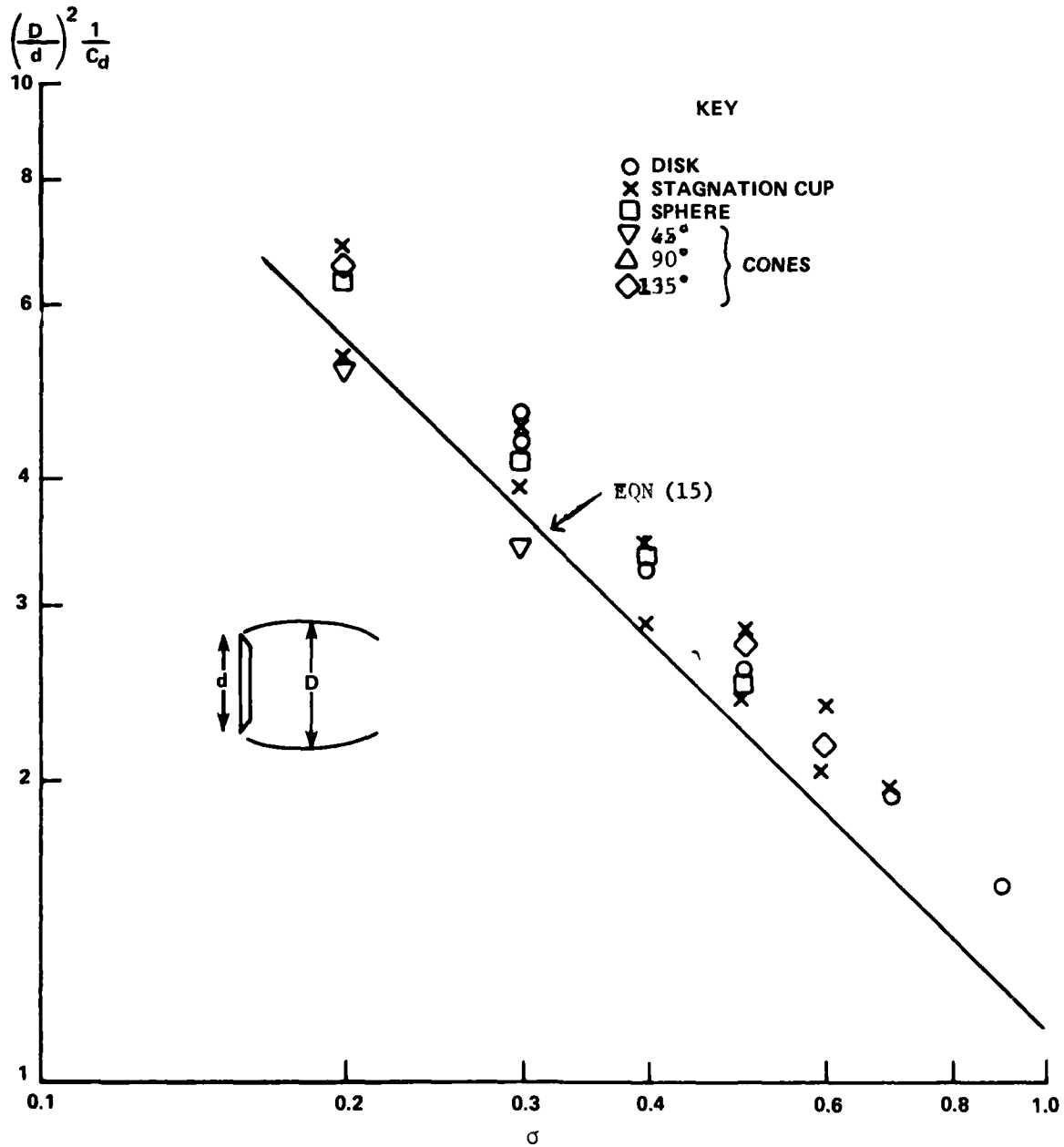


FIG. 5 CAVITY DIAMETER DATA - ROUSE AND McNOWN REF (7)

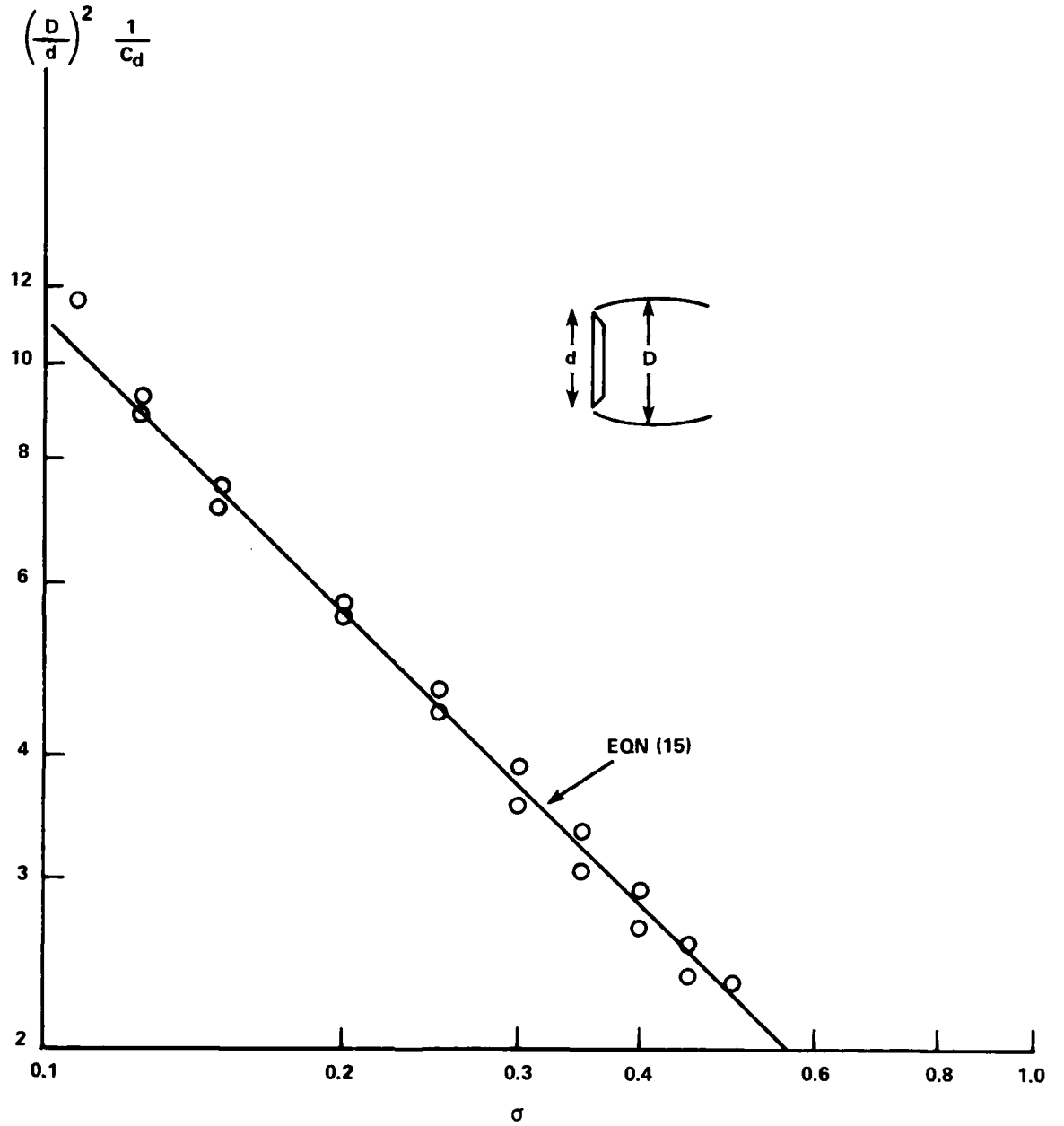


FIG. 6 CAVITY DIAMETER DATA FOR DISKS - EISENBERG-POND REF (8)

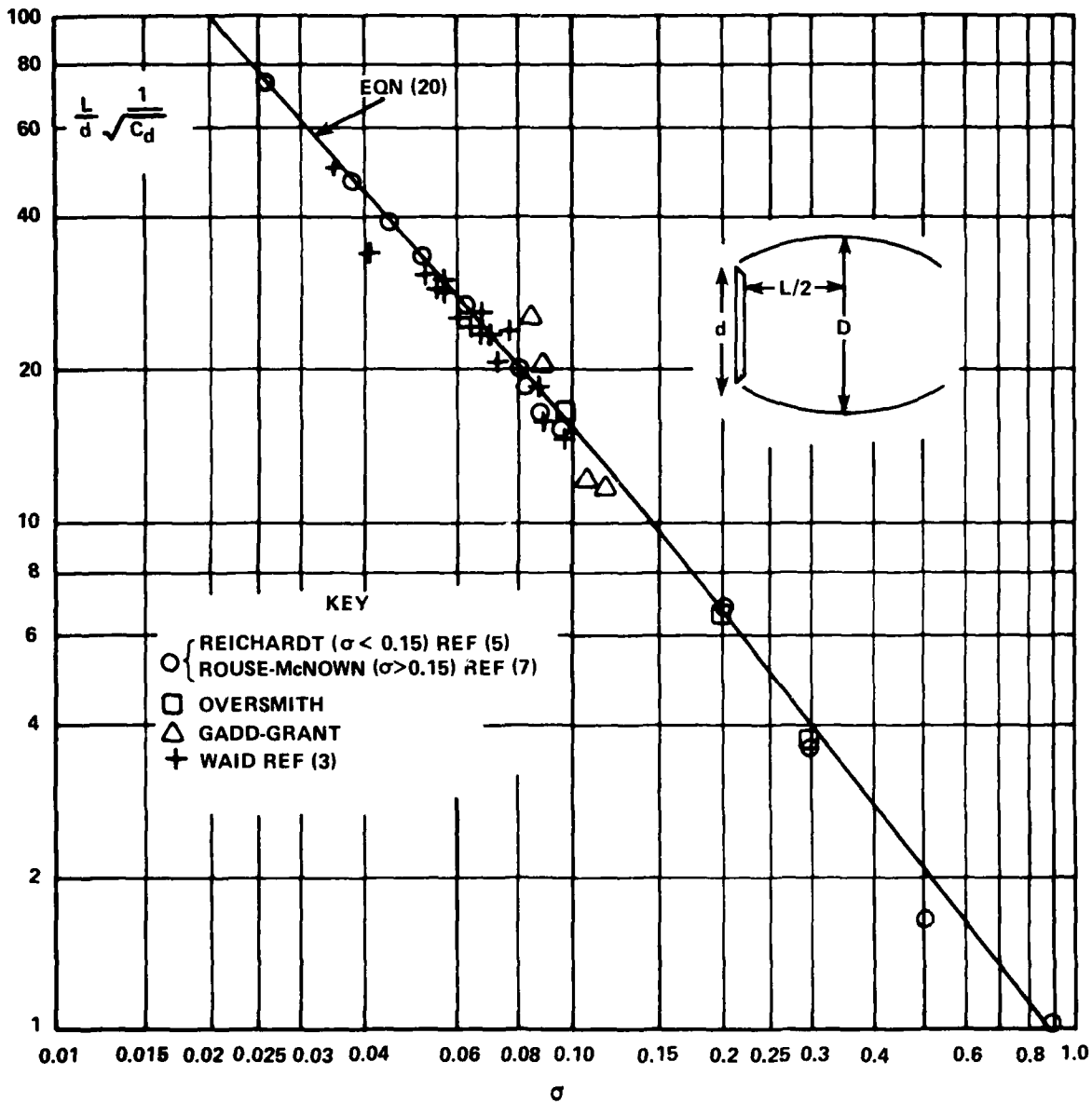


FIG. 7 SCALED LENGTH OF CAVITIES DUE TO A DISK

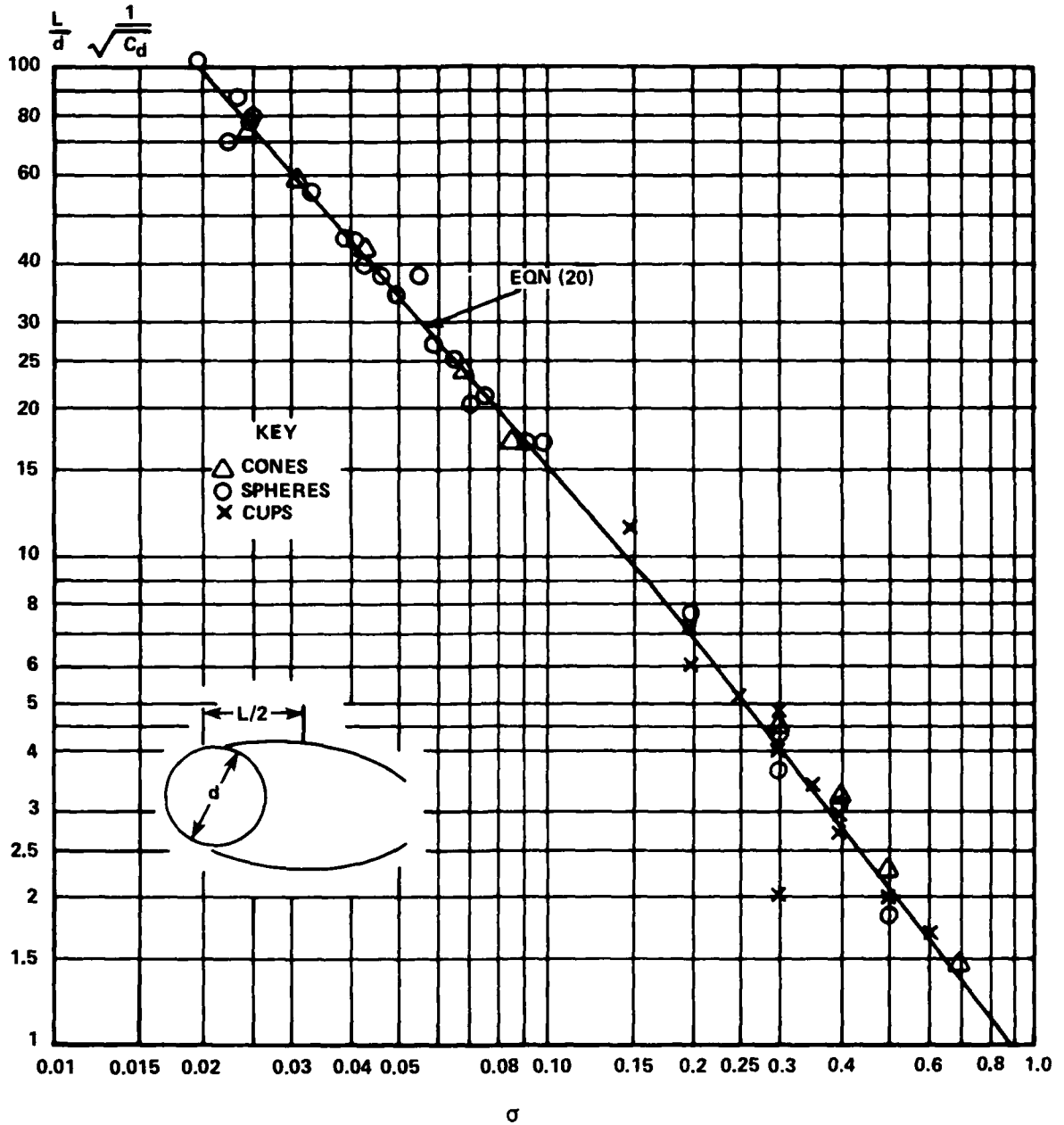


FIG. 8 LENGTH OF CAVITIES FOR VARIOUS NOSE SHAPES

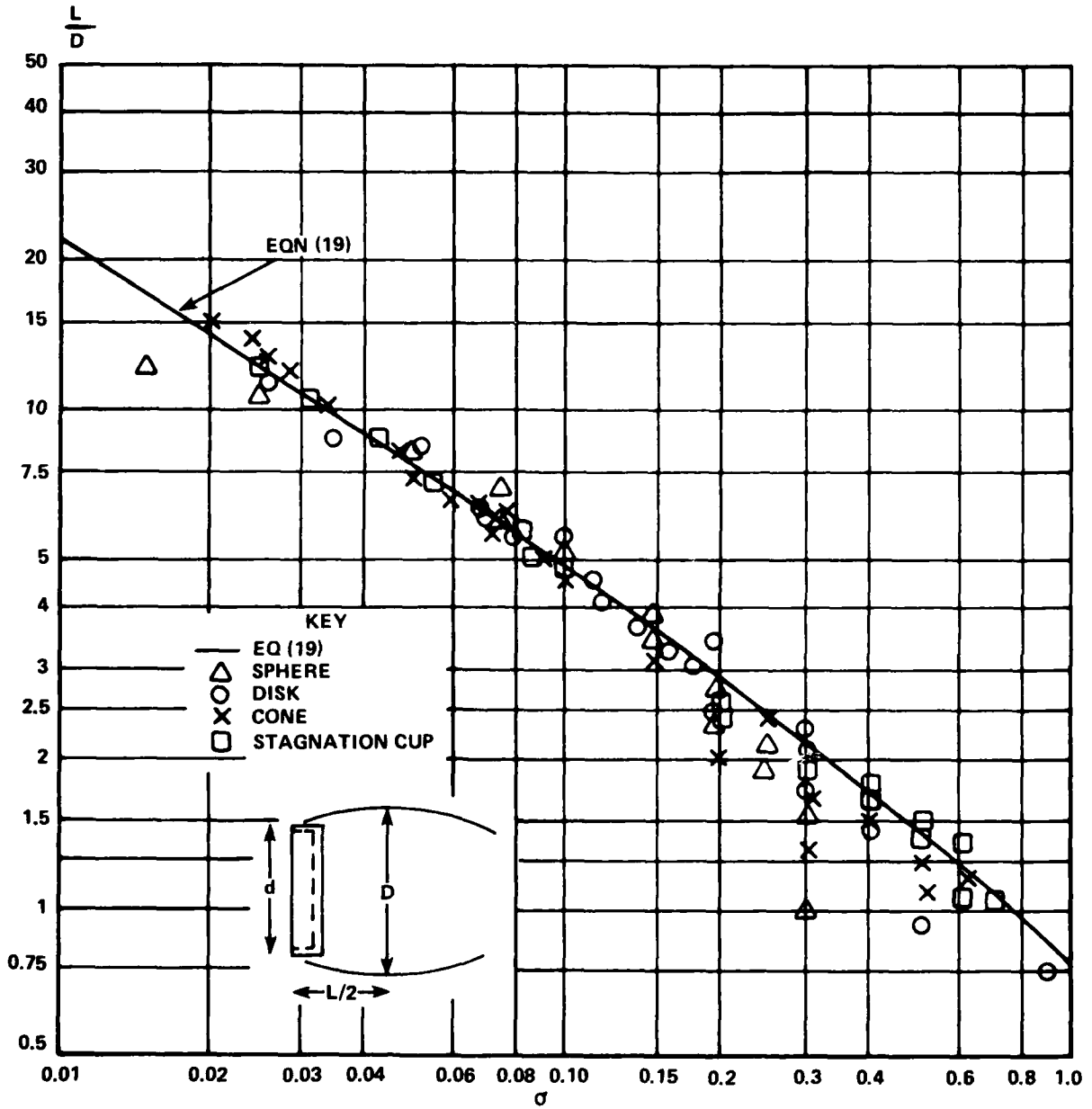


FIG. 9 EXPERIMENTAL L/D DATA

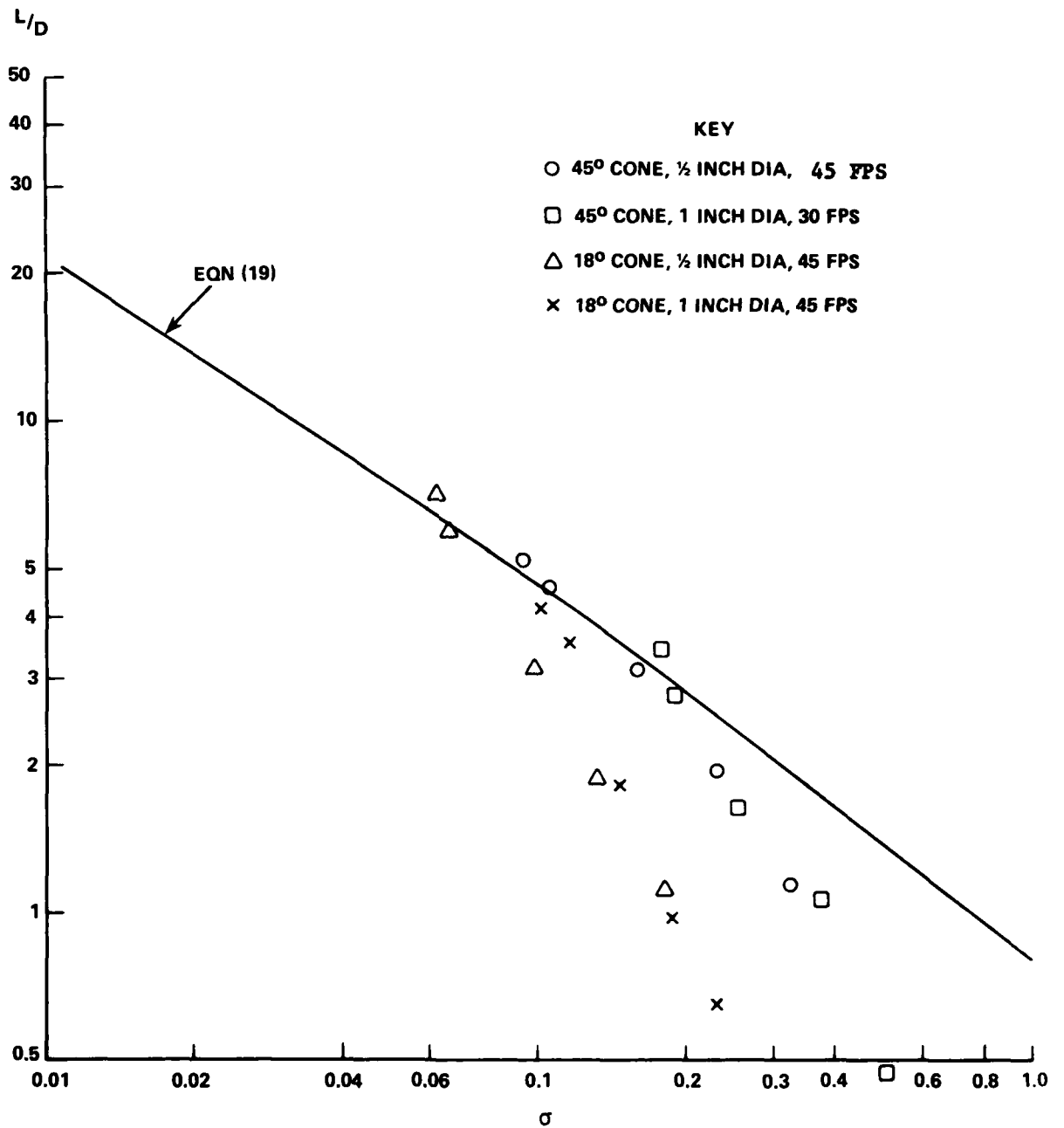


FIG. 10 EXPERIMENTAL L/D DATA - ARL, REF. (1)

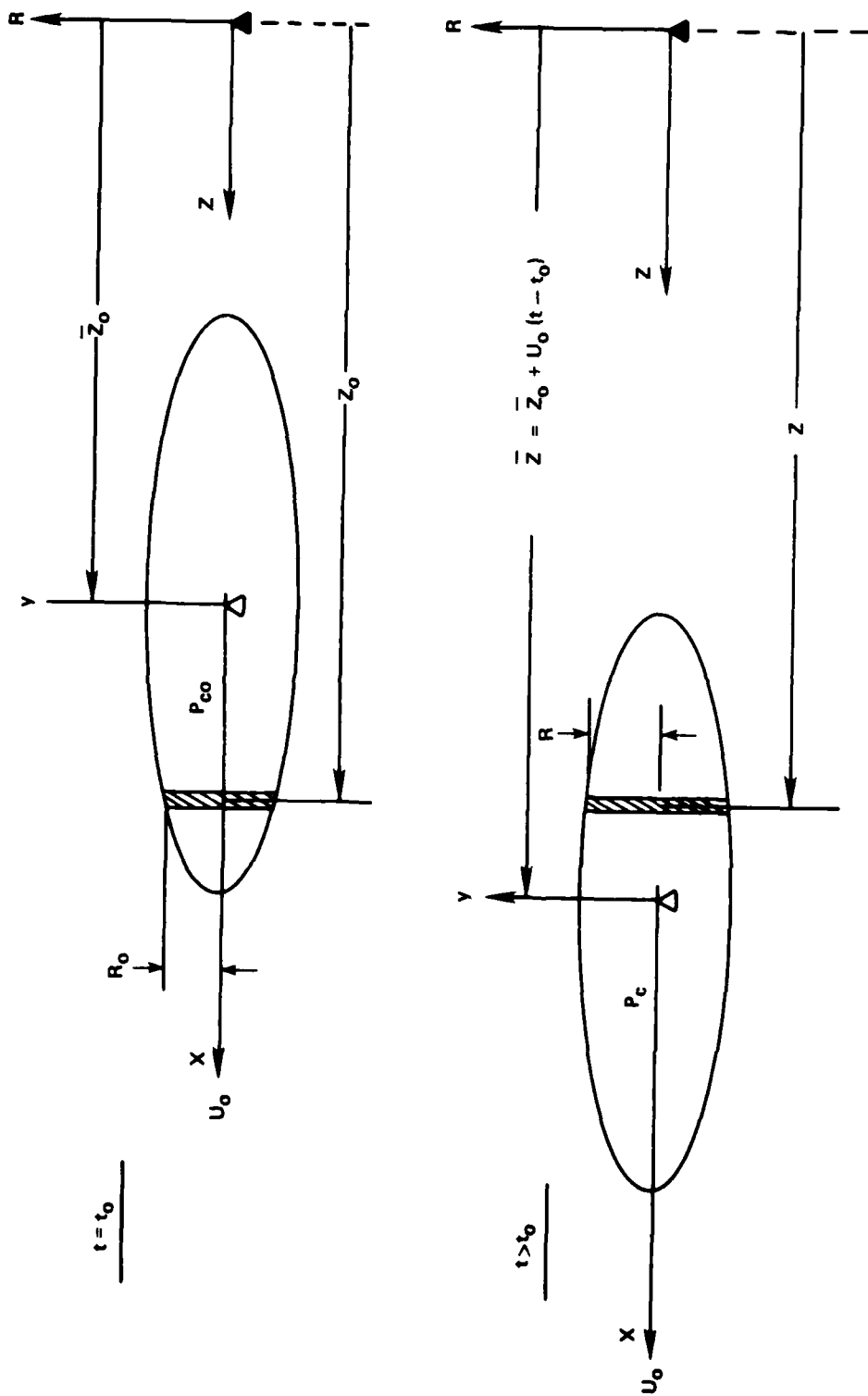


FIG. 11 INERTIAL AND BODY AXIS

DISTRIBUTION

Copies

Commander
Naval Air Systems Command
Washington, D. C. 20362
Attn: AIR-530133A
AIR-53712A
AIR-350D
AIR-350
AIR-350B
AIR-030

Commander
Naval Sea Systems Command
Department of the Navy
Washington, D. C. 20362
Attn: SEA-09G32
SEA-03
SEA-0351
SEA-03512
SEA-0372
SEA-054
SEA-05121
PMS-0647

2

SEA-03B
Office of Naval Research
Department of the Navy
Arlington, Virginia 22217
Attn: ONR-438
ONR-439
ONR-463

Director
Defense Research and Engineering
The Pentagon
Washington, D. C. 20301

Defense Documentation Center
Cameron Station
Alexandria, Virginia 22314

12

Director of Research
National Aeronautics and Space Administration
600 Independence Avenue Southwest
Washington, D. C. 20546

Copies

NASA Scientific and Technical Information Facility
Post Office Box 33
College Park, Maryland 20740

2

Superintendent
U.S. Naval Postgraduate School
Monterey, California 93940
Attn: Library

Commanding Officer
U.S. Naval Air Development Center
Warminster, Pennsylvania 18974
Attn: NADC Library

Director
U.S. Naval Research Laboratory
Washington, D. C. 20390
Attn: Library

2

Commanding Officer
Naval Ship Research and Development Center
Bethesda, Maryland 20084
Attn: Code 154
Code 1541
Code 1556
Code 5613

Commander
Naval Undersea Center
San Diego, California 92132
Attn: Dr. A. Fabula
Dr. J. Hoyt

Commanding Officer
Naval Underwater Systems Center
Newport, Rhode Island 02840
Attn: J. F. Brady
W. A. McNally
R. H. Nadolink

Commander
Naval Weapons Center
China Lake, California 93555
Attn: Library

2

Harry Diamond Laboratories
Washington, D. C. 20438
Attn: Harry Davis
Library

U.S. Army Ballistic Research Laboratories
Aberdeen Proving Ground, Maryland 21105
Attn: Library

National Aeronautics and Space Administration
George C. Marshall Space Flight Center
Huntsville, Alabama 35812
Attn: Library

National Aeronautics and Space Administration
Langley Research Center
Langley Station
Hampton, Virginia 23365
Attn: Library

National Aeronautics and Space Administration
Lewis Research Center
21000 Brookpark Road
Cleveland, Ohio 44135
Attn: Library

Director
Alden Research Laboratories
Worcester Polytechnic Institute
Holden, Massachusetts 01520

2

Applied Physics Laboratory
The Johns Hopkins University
Johns Hopkins Road
Laurel, Maryland 20810
Attn: Document Librarian

2

Applied Research Laboratory
The Pennsylvania State University
Post Office Box 30
State College, Pennsylvania 16801
Attn: Dr. Blaine R. Parkin
Dr. J. W. Holl

AVCO Everett Research Laboratory
2585 Revere Beach Parkway
Everett, Massachusetts 02149
Attn: Library

Copies

Battelle Memorial Institute
505 King Avenue
Columbus, Ohio 43201
Attn: Library

The Boeing Company Aerospace Library
Post Office Box 3999
Seattle, Washington 98124

Garfield Thomas Water Tunnel Library
The Pennsylvania State University
Institute for Science and Engineering
Applied Research Laboratory
Post Office Box 30
State College, Pennsylvania 16801

General Electric Company
Post Office Box 8555
Philadelphia, Pennsylvania 19101
Attn: MSD Library

Hydronautics, Incorporated
Pindell School Road
Laurel, Maryland 20810
Attn: Mr. Philip Eisenburg

2

Iowa Institute of Hydraulic Research
State University of Iowa
Iowa City, Iowa 52240
Attn: Dr. J. F. Kennedy

2

Jet Propulsion Laboratory
4800 Oak Grove Drive
Pasadena, California 91103
Attn: Library

Lockheed Missiles and Space Company
Department 57-24, Building 150
P.O. Box 504
Sunnyvale, California 94088
Attn: Robert Waid

2

Los Alamos Scientific Laboratory
Post Office Box 1663
Los Alamos, New Mexico 87544
Attn: Report Library

Sandia Laboratories
Albuquerque, New Mexico 87115
Attn: Mr. A. Stephenson
Library

Director
Southwest Research Institute
Department of Mechanical Sciences
San Antonio, Texas 78206
Attn: Library

Director
Saint Anthony Falls Hydraulic Laboratories
University of Minnesota
Minneapolis, Minnesota 55455
Attn: Prof. E. Silberman

The Catholic University of America
Washington, D. C. 20017
Attn: Dr. C. C. Chang

Colorado State University
Fort Collins, Colorado 80521
Attn: Civil Engineering Hydraulic Laboratory

California Institute of Technology
Pasadena, California 91109
Attn: Dr. Milton S. Plesset
Dr. Allan J. Acosta

University of Maryland
College Park, Maryland 20742
Attn: Dr. Dirse W. Sallet
Dr. Clifford L. Sayer
Dr. John D. Anderson

Massachusetts Institute of Technology
Cambridge, Massachusetts 02139
Attn: Dr. D. F. F. Harleman

TO AID IN UPDATING THE DISTRIBUTION LIST
FOR NAVAL SURFACE WEAPONS CENTER, WHITE
OAK LABORATORY TECHNICAL REPORTS PLEASE
COMPLETE THE FORM BELOW:

TO ALL HOLDERS OF NSWC/WOL/TR 76-114
by Charles W. Smith Code WA-42
DO NOT RETURN THIS FORM IF ALL INFORMATION IS CURRENT

A. FACILITY NAME AND ADDRESS (OLD) (Show Zip Code)

NEW ADDRESS (Show Zip Code)

B. ATTENTION LINE ADDRESSES:

C.

REMOVE THIS FACILITY FROM THE DISTRIBUTION LIST FOR TECHNICAL REPORTS ON THIS SUBJECT.

D.

NUMBER OF COPIES DESIRED _____

**DEPARTMENT OF THE NAVY
NAVAL SURFACE WEAPONS CENTER
WHITE OAK, SILVER SPRING, MD. 20910**

**OFFICIAL BUSINESS
PENALTY FOR PRIVATE USE, \$300**

**POSTAGE AND FEES PAID
DEPARTMENT OF THE NAVY
DOD 316**



**COMMANDER
NAVAL SURFACE WEAPONS CENTER
WHITE OAK, SILVER SPRING, MARYLAND 20910**

ATTENTION: CODE WA-42